

Separations Via Radial Flow Chromatography in Compacted Particle Beds

Richard G. Rice and Brian K. Heft

Dept. of Chemical Engineering, Louisiana State University, Baton Rouge, LA 70803

Tightly compressed beds of sorbent powders have recently been studied by comparing theoretical with experimental impulse responses of a single solute in a radially flowing inert gas (helium) (Yee, 1987; Rice et al., 1990; Rice and Heft, 1990). These preliminary studies have highlighted the difficulties in radial flow chromatography (RFC) in attaining perfectly symmetrical flow patterns if slight packing nonuniformities exist (Yee, 1987). In the early literature (Hopf, 1947), flow uniformity was achieved by spinning the packed bed in a so-called chromatofuge. This rather large scale spinning basket was used for liquid separations. More recently, Rice (1982) foreshadowed RFC as a small-scale analytical tool, and developed the following dispersion-free theory to predict impulse response behavior, where Table 1 defines the time, θ , and length, x , scales for either axial or radial flow:

$$\frac{C(x, \theta)}{C_o} = \sqrt{\frac{Kx}{\theta \xi^2}} \exp \left[- \left(\frac{Kx + \theta}{\xi} \right) \right] I_1 \left(\sqrt{\frac{4Kx\theta}{\xi^2}} \right) \quad (1)$$

The parameter ξ accounts for combined film and intraparticle resistance.

Subsequent work (Rice et al., 1990) showed in fact that particle-phase resistance was not the primary dissipative effect, but that radial dispersion controlled band broadening. In more recent work (Rice and Heft, 1990), it was proposed that radial dispersion was mainly molecular in origin, as evidenced by comparing single-solute response curves with an analytical solution to the convective-dispersive theory. These results indicated, for practical flow rates, that Taylor-type dispersion, which depends on fluid velocity, was small relative to molecular diffusion. This was not altogether unexpected, for lightly held solutes (methane) in tightly packed beds of small particles, since compression should reduce the effective flow pore size through the interstices, and radial dispersion should be mainly molecular in origin. Such may not be the case for liquids in RFC, since Taylor dispersion varies as $D^T \sim (1/48) (R_H^2 U^2 / D^o)$ and molecular diffusivity, D^o , is quite small. Thus, for

liquids it is even more important to reduce flow pore size, expressed here as hydraulic radius, $R_H = (d_p/6) \epsilon / (1 - \epsilon)$. Researchers studying high-pressure liquid chromatography (HPLC) (axial flow) tend to do this by reducing particle size, d_p , yet it is easy to see that reducing voidage, ϵ , accomplishes the same end. Such highly compacted media are used in paper and thin-layer chromatography, the dynamics for which have been put forth in a series of theoretical papers (Rachinskii, 1968; Rachinskii and Inchin, 1968, 1970; Inchin and Rachinskii, 1968, 1973a, b) for negligible radial diffusion.

Convective-Diffusion Theory

An analytical solution to forecast impulse response in RFC in the presence of dispersion has recently been published (Rice and Heft, 1990), which is the solution of the dynamic material balance equation:

$$(a - D) \frac{1}{r} \frac{\partial C}{\partial r} + \frac{\partial C}{\partial t} + \frac{1}{\eta} \frac{\partial q}{\partial t} = D \frac{\partial^2 C}{\partial r^2} \quad (2)$$

The solution given was applicable for negligible intraparticle resistance, $\xi \ll 1$, and linear adsorption:

$$q = KC \quad (3)$$

Dispersion in the radial fluid flow direction is the only dissipative effect, hence for outward flow the normalized exit response was shown to be:

Table 1. Time and Length Scales in Eq. 1 (Rice, 1982; Yee, 1987)

Flow Config.	Length Scale, x	Rel. Time Scale, θ
Axial	$\frac{z}{(\eta \cdot v)}$	$t - \frac{z}{v}$
Radial	$\frac{1}{2a\eta} (r^2 - R_1^2)$	$t - \frac{1}{2a} (r^2 - R_1^2)$

Correspondence concerning this paper should be addressed to R. G. Rice. B. K. Heft is with Air Products, Inc., St. Gabriel, LA 70776.

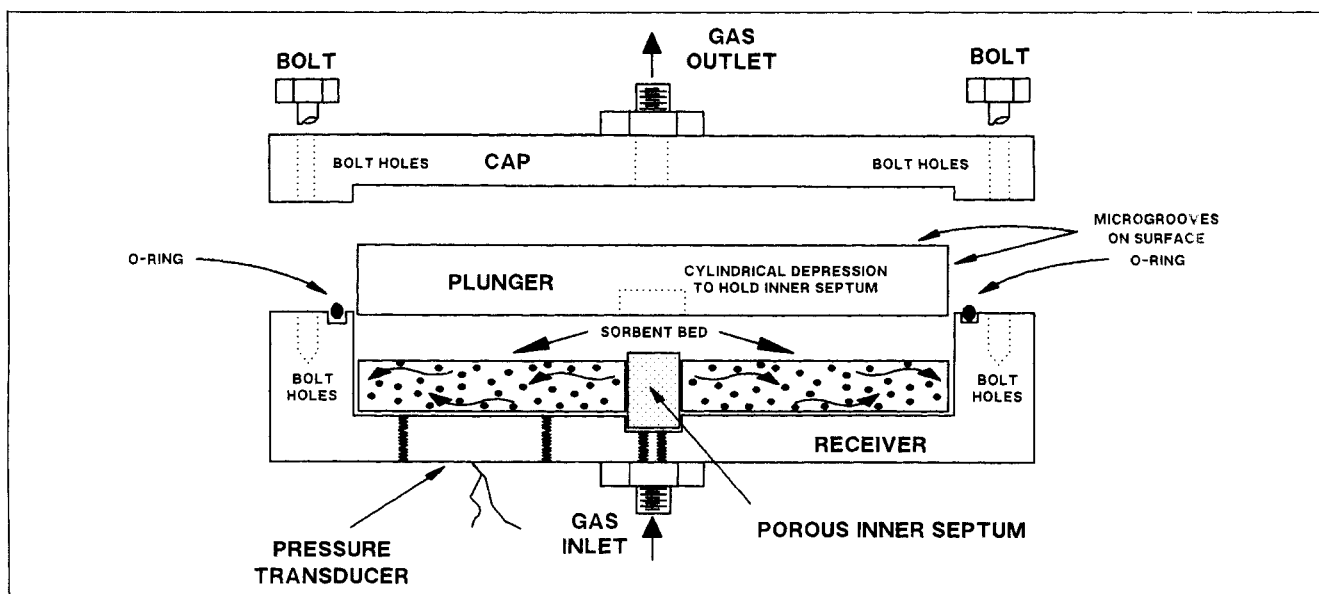


Figure 1. Cross-sectional view of MARK III RFC.

$$C_{Norm} = \sum_{n=1}^{\infty} \frac{\lambda_n}{J_p(\lambda_n)} \exp(-\lambda_n^2 \tau) / \sum_{n=1}^{\infty} \frac{\lambda_n^{p-2}}{J_p(\lambda_n)} \quad (4)$$

where

$$J_{p-1}(\lambda_n) = 0 \quad (5)$$

and it was stipulated that the inner septum, Figure 1, is small enough to be treated as a point source (Rice and Heft, 1990). Inchin and Rachinskii (1973) also studied Eq. 2, apparently for applications toward radial paper chromatography. They obtained an exact solution for the special case of $p = 1/2$ in an infinite sheet, and also deduced an approximate solution for short contact time. No experiments were reported.

The solution has some interesting properties, not the least of which is the appearance of a Peclet number as the order of a Bessel function, that is,

$$p = \frac{a}{2D} = \frac{Q}{4\pi h e D} \quad (6)$$

where Q denotes volumetric flow rate, and h is the bed thickness.

For flow from the periphery inward toward the centerline (inward flow), it is easy to show (Heft, 1991) that the same solution obtains by everywhere replacing p with $(p + 1)$ in Eqs. 4 and 5. This arises because the velocity vector is negative (anti- r direction). This result suggests, Figure 2, that inward flow should sustain slightly sharper peaks than outward flow, everything else being equal. Nonetheless, there are practical reasons for using outward flow, not the least of which is the ease of obtaining uniformity in the injected pulse. It is also abundantly clear that the most practical (future) configuration is a multiple of two-layered beds, so that entrance (injection) and exit (measurement) both lie along the bed centerline.

The effects of Peclet number, p , on exit response curves

(outflow) are illustrated in Figure 3. The placement and shapes of these real-time response curves are uniquely determined by the Peclet number and the system time constant:

$$\tau_c = R_2^2 \frac{K + \eta}{D \cdot \eta} \quad (7)$$

where the capacitance ratio η can be made arbitrarily small (up to a limit; Cooper and Eaton, 1962) by high bed compression.

Experimental Response Curves

Figure 1 illustrates the third in a series of design modifications, henceforth referred to as MARK III, and differs from the previous prototype (Rice and Heft, 1990) in the way gas is collected at the outer perimeter and routed back to the centerline for subsequent composition detection. Previously,

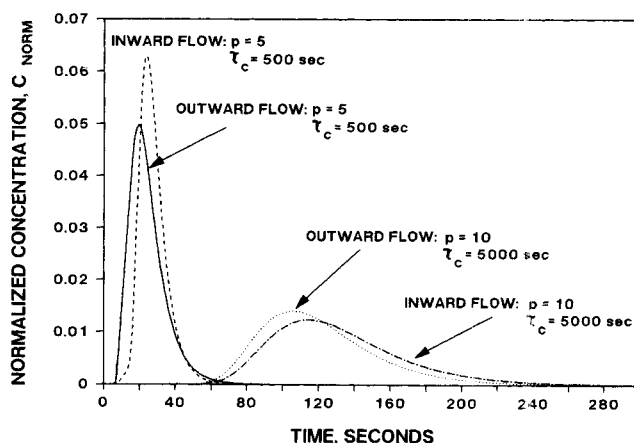


Figure 2. Comparison of outflow with inflow impulse response.

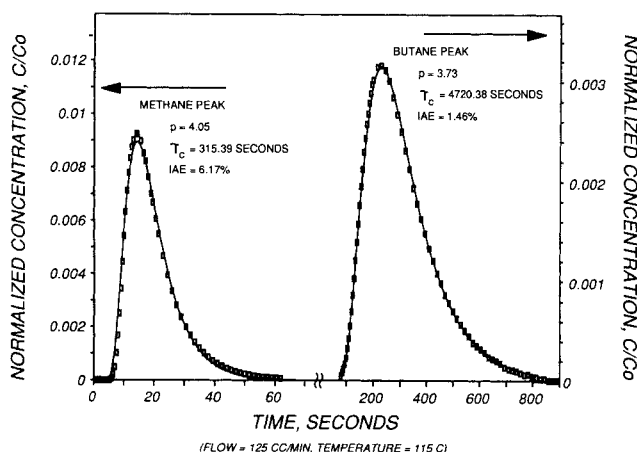


Figure 3. Experimental RFC response curves for methane-butane at 115°C.

□ exp.; — theory, Eq. 4

a porous bronze outer septum was used to collect and route gases. In an effort to reduce hold-up, this has been replaced by fine microgrooves impressed on the outer walls and top of the compression piston as indicated in Figure 1. These grooves were designed to be smaller than the smallest particle size making up the bed. Twenty-six V-shaped grooves 0.15 mm wide and deep were used in the MARK III design.

The sorbent powder consisted of sieved 100-120 mesh ($d_p \approx 0.15$ mm) particles of Alcoa grade F-1 alumina, which was added to the receiver as a slurry in heptane. Slow evaporation under heat and vacuum produced an initially flat and uniform bed. Next, the plunger shown in Figure 1 was placed on top of the bed and subjected to compression by a hydraulic press (Jet Hydraulic) to a pressure of about 69×10^3 kPa (10,000 psi). Our previous efforts used the bolt-on cap to effect compression, but this produced compression, measured by imbedded transducer, of only about 34.5×10^3 kPa (5,000 psi). Following compression, the cap was bolted in place and the bed was conditioned for several days at 150°C in a standard chromatograph oven (Hewlett-Packard 5890) with continuous helium passage. The packed bed dimensions were 76.2 mm (3

in) OD, 6.4 mm (1/4 in) ID, with a packed height of 4.76 mm (3/16 in).

Measurement of bed pressure-drop flow characteristics along with the radial flow equivalent of the Blake-Kozeny equation (Yee, 1987):

$$\Delta P = \frac{150\mu}{d_p^2} \frac{(1-\epsilon)^2}{\epsilon^3} \frac{Q}{2\pi h} \ln \frac{R_2}{R_1} \quad (8)$$

allowed the dynamic voidage to be roughly estimated at about 6 to 8%. We suspect this value is significantly deflated, possibly owing to smaller particles clogging some of the microgrooves, hence pressure drops were greatly inflated (max ~ 16 psi) relative to the earlier prototype (Rice and Heft, 1990). However, we show next that uncertainty in this voidage had little bearing on the rationalization of parameter ratios.

Response curves for 25:75 methane-butane mixture at 115°C are shown in Figure 3, along with values of the fitted parameters p and τ_c . It is useful to inspect the values of these respective ratios, since

$$\frac{p_{CH_4}}{p_{C_4H_{10}}} = \frac{D_{C_4H_{10}}}{D_{CH_4}} \quad (9)$$

and

$$\frac{\tau_c(CH_4)}{\tau_c(C_4H_{10})} = \frac{K_{CH_4} + \eta}{K_{C_4H_{10}} + \eta} \frac{D_{C_4H_{10}}}{D_{CH_4}} \quad (10)$$

Furthermore, since it is always true that $K \gg \eta$, especially for compressed beds, then Eq. 10 can be approximated by

$$\frac{\tau_c(CH_4)}{\tau_c(C_4H_{10})} \approx \frac{K_{CH_4}}{K_{C_4H_{10}}} \frac{D_{C_4H_{10}}}{D_{CH_4}} = \frac{K_{CH_4}}{K_{C_4H_{10}}} \frac{p_{CH_4}}{p_{C_4H_{10}}} \quad (11)$$

so that the uncertain ratio $\eta = \epsilon/(1-\epsilon)$ is eliminated as a parameter. The values for τ_c and p in Figure 3 thus yielded the following ratio for Henry's constants

$$\left(\frac{K_{CH_4}}{K_{C_2H_{10}}} \right)_{radial} \approx 0.062 \quad (12)$$

which is essentially independent of the uncertain measurement of voidage using pressure-drop measurement.

If dispersion is controlled by molecular diffusivity, then the expected ratio of diffusivities can be estimated from the Slatery-Bird relation (Bird et al., 1960):

$$\frac{D_{C_4H_{10}}^0}{D_{CH_4}^0} = \left(\frac{T_{c|CH_4}}{T_{c|C_4H_{10}}} \right)^{\frac{1.823}{2}} \cdot \left(\frac{M_{CH_4}}{M_{C_4H_{10}}} \cdot \frac{M_{C_4H_{10}} + M_{He}}{M_{CH_4} + M_{He}} \right)^{\frac{1}{2}} \quad (13)$$

This relation forecasts a molecular ratio of 0.445, while the parameter estimation of the response data yielded a ratio of 1.09. This can be explained in part by Taylor dispersion effects. For adsorbing species, Dayan and Levenspiel (1968, 1969) have derived a rather elegant extension of Taylor diffusion for conditions of complicated pore structure and surface adsorption effects. An abbreviated form of their result is:

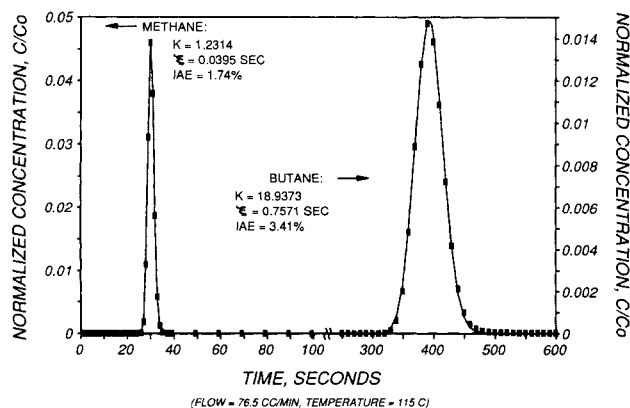


Figure 4. Experimental response curves for axial flow (packed tube) bed.

Methane-butane, 115°C, in He. flow 76.5 cm³/min
■ exp.; — theory, Eq. 1

$$D = D^o + f(K) \frac{R_H^2 U^2}{48 \cdot D^o} = D^o + D^T \quad (14)$$

where $f(K)$ is a polynomial function of the linear adsorption coefficient K . Thus, the combination of strong adsorption and low values of molecular diffusivity—precisely the case for butane—can lead to significant Taylor dispersion effects. Such effects can be reduced by using elevated temperature (reducing K) and by increased compaction (reducing R_H).

To provide an independent evaluation of Henry's constants, we performed response tests on a standard axial flow chromatography (AFC) packed tube as illustrated in Figure 4. The 3.2 mm (1/8 in) ID tube was packed with the same F-1 alumina to a length of 1,829 mm (72 in). Equation 1 was used to fit the data at 115°C, taking K and ξ to be unknown parameters; the definitions of time and length scales for axial flow conditions are given in Table 1. The fitted parameters are given in Figure 4. Flow pressure-drop measurements along with the Blake-Kozeny equation gave an estimate of 30% for voidage. The ratio of the Henry constants is thus seen to be

$$\left(\frac{K_{CH_4}}{K_{C_4H_{10}}} \right)_{axial} \approx 0.065 \quad (15)$$

which is very close indeed to the ratio of values obtained independently for the radial flow case. We take special note of the very small deviation of theory and experiment (IAE < 4%), which lends strong support to Eq. 1 when axial dispersion is unimportant. Details of the nearly one hundred experiments on RFC and AFC can be found elsewhere (Heft, 1991).

Acknowledgment

This research was supported by the National Science Foundation, Grant No. CBT-8804705, and by support from Air Products Inc. to B. K. Heft. A patent application has been filed and is pending (430,495).

Notation

- a = $Q/(2\pi h\epsilon)$, volume flux, m²/s
- C = solute composition in flowing phase, mol/m³
- D^o = molecular diffusivity, m²/s
- D = radial dispersion coefficient, m²/s
- D_p = particle phase effective diffusivity, m²/s
- D^T = Taylor dispersion coefficient, m²/s
- d_p = particle diameter, m
- h = bed thickness, m
- IAE = integral absolute error
- $I_1(x)$ = modified Bessel function
- $J_p(x)$ = Bessel function of first kind, order p
- k_m = mass transfer coefficient, m/s
- K = linear adsorption constant (Henry's constant)
- M = molecular weight
- p = $a/(2D)$, Peclet number
- q = average solid phase composition, mol/m³
- Q = volumetric flow rate, m³/s
- r = radial coordinate of bed, m
- R_1 = inner bed radius, m

- R_2 = outer bed radius, m
- R_H = hydraulic radius of interstitial flow pore, m
- t = time, s
- T_c = critical temperature, K
- U = linear velocity through interstices, m/s
- v = axial flow interstitial velocity, m/s
- x = length scale, Table 1, s
- z = axial flow length coordinate, m

Greek letters

- ϵ = bed voidage
- ξ = particle resistance $\left(= \frac{K d_p}{6 k_m} + \frac{d_p^2}{60 D_p} \right)$, s
- η = capacity ratio, $\epsilon/(1 - \epsilon)$
- μ = fluid viscosity, Pa·s
- Θ = relative time scale, Table 1, s
- τ_c = system time constant, Eq. 7, s
- τ = dimensionless time, t/τ_c

Literature Cited

- Bird, R. B., W. E. Stewart, and E. N. Lightfoot, *Transport Phenomena*, Wiley, New York (1960).
- Cooper, A. R., and L. E. Eaton, "Compaction Behavior of Several Ceramic Powders," *J. Am. Ceramic Soc.*, **45**, 97 (1962).
- Dayan, J., and O. Levenspiel, "Longitudinal Dispersion in Packed Beds of Porous Adsorbing Solids," *Chem. Eng. Sci.*, **23**, 1327 (1968).
- Dayan, J., and O. Levenspiel, "Dispersion in Smooth Pipes with Adsorbing Walls," *Ind. Eng. Chem. Fundam.*, **8**, 840 (1969).
- Heft, B. K., "Radial Flow Chromatography in Compressed Pancake-Shaped Beds," PhD Diss., Louisiana State Univ. (1991).
- Hopf, P. P., "Radial Chromatography in Industry," *Ind. Eng. Chem.*, **39**, 938 (1947).
- Inchin, P. A., and V. V. Rachinskii, "Theory of Radial-Cylindrical Sorption Dynamics. 2: Dynamics of Sorption During Filtration Toward the Axis of a Cylindrical Layer of Sorbent," *Fuss. J. Phys. Chem.*, **42**(2), 278 (1968).
- Inchin, P. A., and V. V. Rachinskii, "Theory of Radically Cylindrical Sorption Dynamics. 4: Nonequilibrium Frontal Sorption Dynamics for a Linear Isotherm," *Russ. J. Phys. Chem.*, **47**(8), 1159 (1973a).
- Inchin, P. A., and V. V. Rachinskii, "Theory of Radial-Cylindrical Sorption Dynamics. 5: Frontal Equilibrium Sorption Dynamics with Longitudinal Diffusion," *Russ. J. Phys. Chem.*, **47**(9), 1331 (1973b).
- Rachinskii, V. V., "Basic Principles of Radial Chromatography," *J. Chromat.*, **33**, 234 (1968).
- Rachinskii, V. V., and P. A. Inchin, "Theory of Radial-Cylindrical Sorption Dynamics. 1: Fundamental Laws," *Russ. J. Phys. Chem.*, **42**(4), 497 (1968).
- Rachinskii, V. V., and P. A. Inchin, "Theory of Radial-Cylindrical Sorption Dynamics. 3: Steady-State Conditions in Frontal Sorption Dynamics," *Russ. J. Phys. Chem.*, **44**(3), 415 (1970).
- Rice, R. G., "Approximate Solutions for Batch, Packed Tube, and Radial Flow Adsorbers—Comparison with Experiment," *Chem. Eng. Sci.*, **37**, 83 (1982).
- Rice, R. G., and B. K. Heft, "Radial Flow Chromatography in Compressed Pancake-Shaped Beds," *Chem. Eng. Comm.*, **98**, 231 (1990).
- Rice, R. G., B. K. Heft, M. Borie and M. Yee, "Radial Flow Chromatography," *Proc. 3rd Fund. Adsorption Conf.*, Sonthofen (1990).
- Yee, M., "Fluid Mechanics and Transient Mass Transfer for Radial Flow in Pancake-Shaped Packed Beds," MS Thesis, Louisiana State Univ. (1987).

Manuscript received Sept. 13, 1990, and revision received Jan. 14, 1991.